Original Article | Annals of Dermatology 2021;33(6):522-530 • https://doi.org/10.5021/ad.2021.33.6.522

A Clinical and Biochemical Evaluation of a Temperature-Controlled Continuous Non-Invasive Radiofrequency Device for the Treatment of Melasma

Soon-Hyo Kwon, Jung-Im Na[1], Chang-Hun Huh[1], Kyoung-Chan Park[1]

Department of Dermatology, Kyung Hee University Hospital at Gangdong, Kyung Hee University School of Medicine, Seoul, [1]Department of Dermatology, Seoul National University Bundang Hospital, Seoul National University College of Medicine, Seongnam, Korea

Received February 22, 2021
Revised April 1, 2021
Accepted April 2, 2021

Corresponding Author
Kyoung-Chan Park
Department of Dermatology, Seoul National University Bundang Hospital, Seoul National University College of Medicine, 82 Gumi-ro 173beon-gil, Bundang-gu, Seongnam 13620, Korea
Tel: +82-31-787-7311
Fax: +82-31-787-4058
E-mail: gcpark@snu.ac.kr
https://orcid.org/0000-0002-1588-3307

Background: Melasma shows characteristic histological features of photoaged skin.
Objective: We evaluated the effect of dermal rejuvenation using a temperature-controlled continuous non-invasive radiofrequency (RF) device on melasma.
Methods: Continuous skin heating at the temperature of 43°C for 20 minutes was performed in ten subjects with melasma who underwent 3 tri-weekly RF sessions. Pigmentation was evaluated with Mexameter® and investigator's global assessment (IGA). Immunohistochemical staining and image analysis was performed to evaluate biopsies from melasma skin before and after the treatment.
Results: The lesional melanin index was decreased by 13.7% at week 9. IGA score was improved from 3.50 at baseline to 2.95 at week 9. No significant adverse event was reported. Histologic analysis revealed reduced melanin and increased collagen density and thickness. The expression of procollagen-1 and type IV collagen was increased after the treatment. The number of $p16^{INK4A}$-positive senescent fibroblasts was reduced after the treatment, while the expression of heat shock protein 70 and 90 was increased. Stromal derived factor-1, a senescence-associated anti-melanogenic factor secreted from the fibroblasts, was up-regulated after the treatment, while the level of c-kit was not changed.
Conclusion: Thermal skin stimulation by the temperature-controlled continuous RF device improved melasma through dermal rejuvenation.

Keywords: Fibroblasts, Melanosis, Radiofrequency therapy, Skin aging

INTRODUCTION

Melasma is an acquired pigmentary disorder, which is particularly common in Asian women in their thirties and forties[1]. It appears as bilateral symmetrical light-to-dark brown-colored irregular macules on sun-exposed areas of the skin, especially on the face. Chronic ultraviolet (UV) exposure, genetic predisposition, and sex hormones have been implicated in the pathogenesis of melasma[2]. However, recent evidence supports that melasma is not only a pigmentary disorder, but also a consequence of photoaged skin[3,4]. Histologically, melasma is characterized by solar elastosis, increased vascularization, higher number of mast cells, and disrupted basement membrane, which are characteristic findings of photoaged skin[5]. Therefore, recurrence of melasma is frequently observed despite successful anti-melanogenic treatment[6].

The role of fibroblasts in pigmentation has been studied in several studies. Palmoplantar fibroblasts express a higher level of Dickkopf1 than trunk skin fibroblasts, which suppresses melanogenesis via the inhibition of the Wnt canonical pathway[7,8]. Higher level of neuregulin-1 was expressed in dark skin fibroblasts than in those from lighter skin type, which activates the PI3K and MAPK signaling pathways in melanocytes[9,10]. Fibroblast-derived factors are not only involved in the physi-

ologic pigmentation of the skin, but also in the pigmentary disorders, such as melasma[7,8]. Secreted Frizzle-related protein 2, which is highly expressed in melasma skin, functions as a melanogenic stimulator by activating the Wnt pathway[11]. Similarly, a reduced level of Wnt inhibitory factor-1 in melasma stimulates melanogenesis[12]. Fibroblasts from melasma skin increased the melanogenesis in cultured human melanocytes and artificial skin through the upregulation of nerve growth factor-β[13].

Recent studies highlighted the role of photoaged fibroblasts in the pathogenesis of melasma[14]. Chronic UV exposure causes senescence of the fibroblasts, especially in the upper dermis. Senescent fibroblasts secrete senescence-associated secreted proteins (SASPs), which promotes melanogenesis in melanocytes[15-17]. Therefore, anti-ageing approaches for the rejuvenation of the dermal environment by eliminating or rejuvenating senescent fibroblasts have been introduced to treat melasma. Better therapeutic results were obtained with combination therapy of microneedle radiofrequency (RF) and low-fluence Q-switched Nd:YAG laser than with the low-fluence Q-switched Nd:YAG laser alone in the treatment of melasma[18,19].

In this study, we evaluated the efficacy and safety of temperature-controlled continuous non-invasive RF in treating melasma. We investigated whether the RF treatment was able to reverse the photoaged characteristics observed in melasma histology. Moreover, we examined the expression of heat shock proteins (HSPs) and the secretion of SASPs to demonstrate the effect of the RF treatment and reduced pigmentation.

MATERIALS AND METHODS

Subjects

A total of 10 female volunteers with melasma were enrolled in this study. All subjects had Fitzpatrick skin types III and IV. The mean age was 49.80 years (ranging from 45 to 64 years). Diagnosis was done by physical examination and confirmed by histological findings. Those who underwent any aesthetic medical procedure or used topical depigmenting agent within three months prior to the study were excluded.

RF treatment

Subjects were treated with a bipolar RF device (Forma®; Inmode Inc., Richmond Hill, ON, Canada) three times at a 3-week interval. The treatment areas included both cheeks, lower eyelids, nasolabial folds, and jowls. Prior to the procedure, the treatment areas were gently cleansed with a mild cleanser. After applying ultrasound gel, the probe was gently applied to the treatment areas in small circular motion to uniformly heat the area. With the help of real-time temperature monitoring, the device automatically activated or terminated the delivery of RF energy to maintain target temperature in the treatment areas. The parameters were set at the target temperature of 43°C and energy of 62 mJ. Each subject was treated for 20 minutes per session.

Subjects were scheduled to visit at week 0 (baseline), week 3, week 6, and week 9. At each visit, the melanin index (MI) and erythema index (EI) of the lesions and preauricular area were measured using Mexameter (MX18®; Courage & Khazaka, Köln, Germany). Two blinded, independent dermatologists assessed the overall severity of the disease using a 5-point investigator's global assessment (IGA) scale (5, very severe; 4, severe; 3, moderate; 2, mild; 1, minimal melasma). The IGA score was determined by the median value of IGA from the two dermatologists.

Immunohistochemical analysis

A 2 mm-sized punch biopsy was performed at the darkest melasma lesion at baseline (week 0) and at three weeks after the final treatment (at week 9). The skin samples were stained for hematoxylin and eosin (H&E), Fontana-Masson, and Masson's trichrome to measure the amount of melanin and collagen fibers. Immunohistochemical staining was performed on formalin-fixed, paraffin-embedded tissues. The paraffin sections underwent deparaffinization in a HistoChoice Clearing Agent (Amresco, Solon, OH, USA), rehydration from graded ethanol to distilled water, and antigen retrieval using Trilogy solution (Cell Marque, Rocklin, CA, USA) and a pressure cooker. Nonspecific antibody binding was blocked by normal goat (ab7481; Abcam, Cambridge, UK), donkey (ab7475; Abcam), and chicken (ab7477; Abcam) serums. The primary antibodies used were as follows; procollagen-1, 1:50 (SP1.D8; DSHB, Iowa City, IA, USA); type IV collagen, 1:50 (ab8201; Abcam); CD31, 1:50 (M0823; Dako, Carpinteria, CA, USA); mast cell tryptase, 1:50 (sc-32473; Santa Cruz Biotechnology, Santa Cruz, CA, USA); $p16^{INK4A}$, 1:50 (ab189034; Abcam); HSP47, 1:50 (sc8352; Santa Cruz Biotechnology); stromal derived factor-1 (SDF-1), 1:50 (sc74271; Santa Cruz Biotechnoogy); c-kit, 1:50 (sc1494; Santa Cruz Biotechnology); HSP70 (sc32239; Santa Cruz Biotechnology); HSP90 (ab6536; Abcam). The secondary antibodies were

Alexa Flour® 488 goat anti-mouse immunoglobulin G (IgG) (A11001; Invitrogen, Carlsbad, CA, USA), Alexa Flour® 488 goat anti-rabbit IgG (A11008; Invitrogen), Alexa Flour® 488 chicken anti-mouse IgG (A21200; Invitrogen), Alexa Flour® 488 chicken anti-rabbit IgG (A21441; Invitrogen), Alexa Flour® 488 chicken anti-goat IgG (A21467; Invitrogen), Alexa Flour® 555 donkey anti-mouse IgG (A31570; Invitrogen), Alexa Flour® 555 donkey anti-rabbit IgG (A31572; Invitrogen), and Rhodamine donkey anti-rabbit IgG (sc2092; Santa Cruz Biotechnology). After staining with DAPI (1 μg/ml, 10236276001; Roche, Indianapolis, IN, USA), images were detected using Confocal Laser Scanning Microscope (LSM710; Carl Zeiss, Jena, Germany).

Image analysis

ImageJ version 1.52a (National Institute of Health, Bethesda, ML, USA) was used to evaluate the image signals. The staining intensity of melanin and collagen were determined in the Fontana-Masson and Masson's trichrome stains, respectively. The immunostaining images were analyzed in the most highly labeled areas (hot field) under 200× magnification. For the expression analysis of procollagen-1, mast cell tryptase, $p16^{INK4A}$ and HSP47, the number of procollagen-1-, mast cell tryptase-, $p16^{INK4A}$-, and HSP47-positive cells in the dermis within 200 μm from the epidermal-dermal junction was counted. For the expression analysis of CD31 and SDF-1, the signal intensity in the dermis within 200 μm from the epidermal-dermal junction was evaluated[20]. The signal intensity of type IV collagen was determined in the epidermal-dermal junction.

Statistical analysis

SPSS Statistics 21.0 (IBM Corp., Armonk, NY, USA) was used for all data analyses. Wilcoxon's signed rank test was used to determine the statistical significance. A p-value of less than 0.05 was considered to indicate statistical significance. All results are presented as the mean±standard deviation.

Ethics statement

This study was conducted in accordance with the Declaration of Helsinki and International Conference on Harmonization and Good Clinical Practice Guidelines and was reviewed and approved by the institutional review board of Seoul National University Bundang Hospital (B-1805/466-007). Written informed consents were obtained from all subjects before study enrollment. We received the patient's conset form about publishing all photographic materials.

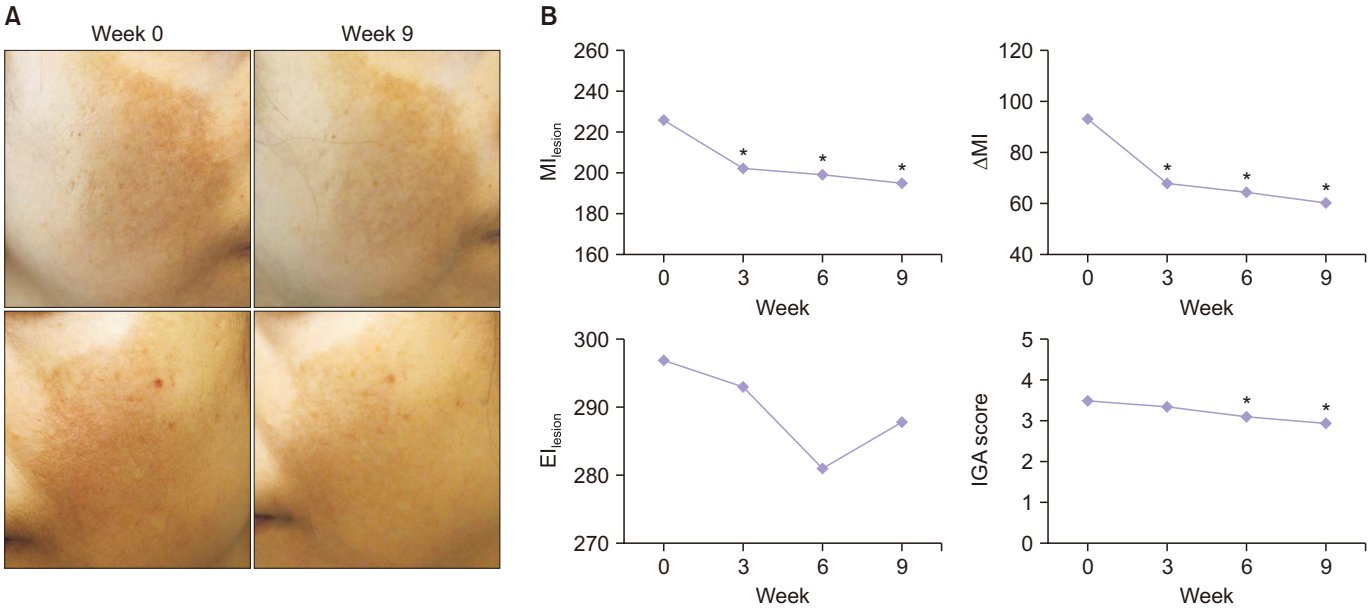

Fig. 1. Radiofrequency (RF) improved the pigmentation in melasma patients. (A) Clinical photographs of a subject at week 0 and 9, who was treated with the RF, showing improvement in pigmentation. (B) The lesional melanin index (MI) and ΔMI (which indicates the difference between the lesional and non-lesional MI) were decreased at week 3, 6, and 9 compared with the baseline. Clinical improvement was also demonstrated by the investigator's global assessment (IGA) score, which improved from 3.50 at week 0 to 2.95 at week 9. No significant change in the erythema index (EI) was observed during the study. *Statistically significance ($p<0.05$).

RESULTS

The radiofrequency treatment improved pigmentation in melasma skin

All subjects showed clinical improvement in pigmentation after the RF treatment (Fig. 1A). The lesional MI at week 3, 6, and 9 were decreased by 10.4%, 11.9%, and 13.7%, respectively, when compared with the baseline (225.73±41.93 at baseline, 202.23±50.04 at week 3, 198.80±48.52 at week 6, and 194.77±52.73 at week 9) (Fig. 1B). To eliminate seasonal variation of skin tone, we also measured the non-lesional MI at the preauricular area, which is exposed to sunlight, but not treated with the RF device. There was no significant change in the non-lesional MI throughout the study (132.53±27.40 at baseline, 134.40±28.23 at week 3, 134.30±28.78 at week 6, and 134.63±28.45 at week 9). The ΔMI, which indicates the difference between the lesional and non-lesional MI, was also decreased at week 3, 6, and 9 compared with the baseline. The clinical improvement was also demonstrated by the IGA score, which improved from 3.50 at week 0 to 2.95 at week 9. Meanwhile, there was no significant change in EI throughout the study.

None of the subjects complained of procedural pain or required anesthesia. Postoperative erythema, which disappeared after a few minutes, was observed in all subjects. Adverse events, including postoperative swelling and tenderness, burn, or postinflammatory hyperpigmentation, were not reported throughout the study period.

The radiofrequency treatment promoted neocollagenesis and restoration of basement membrane in melasma skin

Histologic analysis revealed reduced deposition of melanin after the RF treatment (Fig. 2). In Masson's trichrome stain, elevation of collagen density and thickness was observed in the dermis.

Immunohistochemical study was performed to investigate the effects of RF treatment on the dermis. Increased number of cells expressing procollagen-1 was observed in the dermis after the RF treatment (Fig. 3). Immunostaining for type IV collagen showed that disrupted basement membrane in the melasma skin was restored after the RF treatment. Meanwhile, significant changes in the vascularity and the number of mast cells were not observed in the dermis via the immunostaining for CD31 and mast cell tryptase.

The radiofrequency treatment reduced the number of senescent fibroblasts and increased the expression of HSP70 and HSP90 in melasma skin

We further examined the immunostaining for $p16^{INK4A}$, which is a known senescent cell marker[21]. An increased number of $p16^{INK4A}$-positive fibroblasts was previously reported in the der-

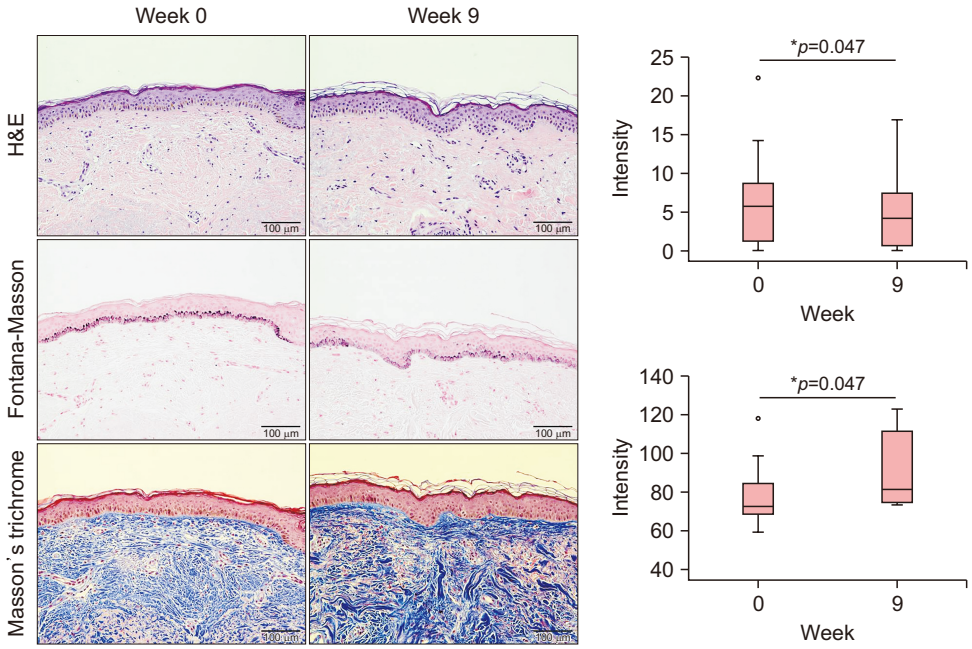

Fig. 2. Histologic analysis revealed reduced deposition of melanin and increased collagen density and thickness after the radiofrequency treatment. Original magnification ×200. *Statistically significance ($p<0.05$).

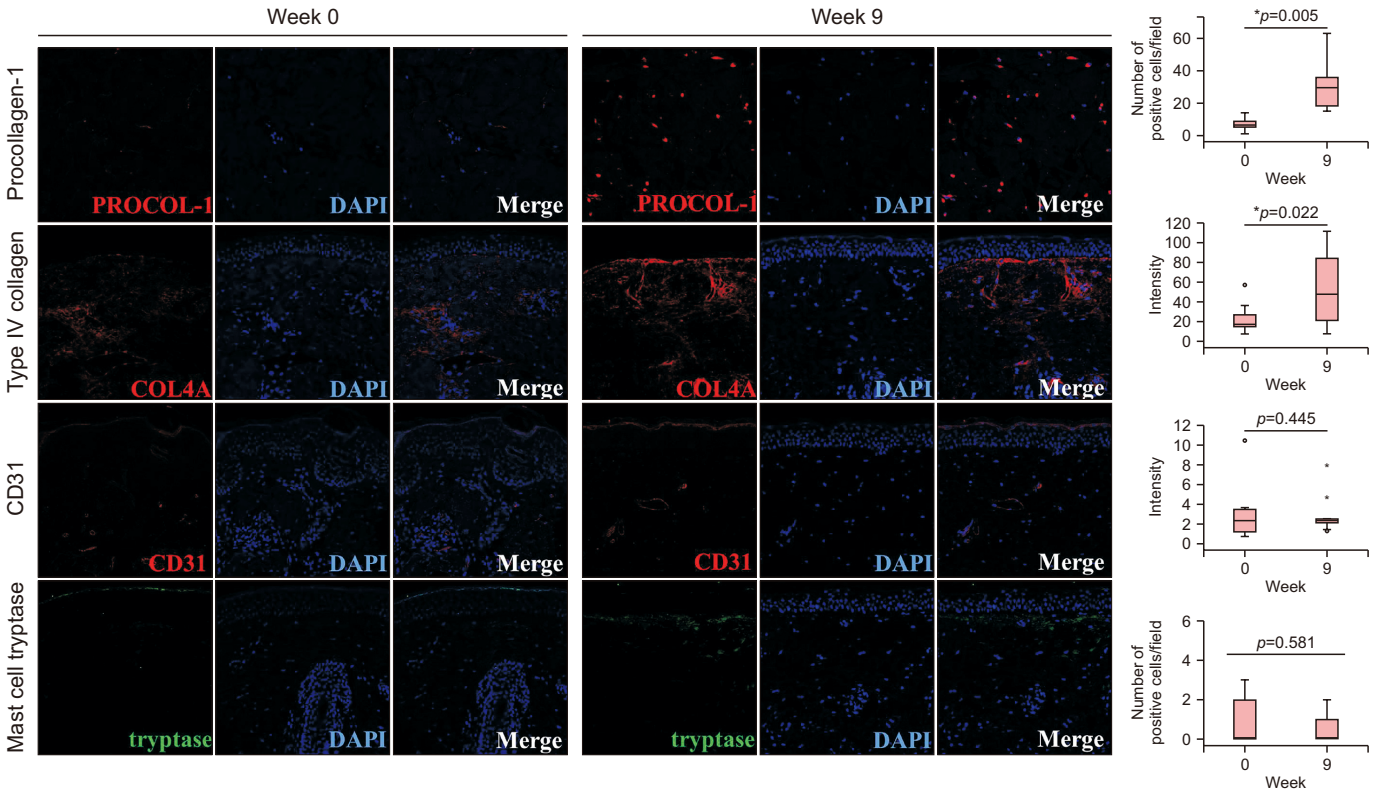

Fig. 3. Radiofrequency (RF) promoted neocollagenesis and restored basement membrane. Increased number of cells expressing procollagen-1 was observed in the dermis after the RF treatment. Immunostaining for type IV collagen showed that disrupted basement membrane in melasma skin was restored after the RF treatment. However, significant changes in the vascularity and the number of mast cells were not observed in the dermis through the immunostaining for CD31 and mast cell tryptase. Original magnification ×200. *Statistically significance ($p<0.05$).

mis of senile lentigo, which is a prototype of photoaged skin[17]. We found a presence of $p16^{INK4A}$-positive cells in the dermis of melasma skin (Fig. 4A). The $p16^{INK4A}$-positive cells were spindle-shaped, and a majority of them were observed in the upper layer of the dermis. Double immunostaining for $p16^{INK4A}$ and HSP47, a collagen-specific molecular chaperone, which is essential for collagen maturation, confirmed that the senescent cells were indeed fibroblasts (Fig. 4B)[22]. After the RF treatment, the number of $p16^{INK4A}$-positive fibroblasts was reduced significantly (Fig. 4C). The mean number of $p16^{INK4A}$-positive fibroblasts per field decreased from 14.1 to 4.4 after treatment. The expression of HSP70 and HSP90 was increased in the dermis of melasma skin after the RF treatment (Fig. 4D).

The radiofrequency treatment increased the secretion of SDF-1

To explain the association between the dermal remodeling and reduced pigmentation, we reviewed the literatures and selected SDF-1 and c-kit as the melanogenic signals from fibroblasts in melasma. A recent study reported the suppressed secretion of SDF-1 in senescent fibroblasts of senile lentigo through DNA methylation[17]. We found that the expression of SDF-1 was down-regulated in the dermis of melasma skin (Fig. 5). However, the RF treatment significantly induced the secretion of SDF-1 in the dermis.

Stem cell factor (SCF) is a fibroblast-derived potent melanogenic cytokine, which binds to the c-kit to activate the extracellular signal-regulated kinase (ERK) pathway in melanogenesis[16,23]. The up-regulated expression of c-kit on melanocytes was reported in melasma skin[24]. However, immunostaining for the c-kit showed no significant change post-RF treatment.

DISCUSSION

Melasma is a photoaging disorder that is characterized by not only pigmentation but also by alterations in the dermal

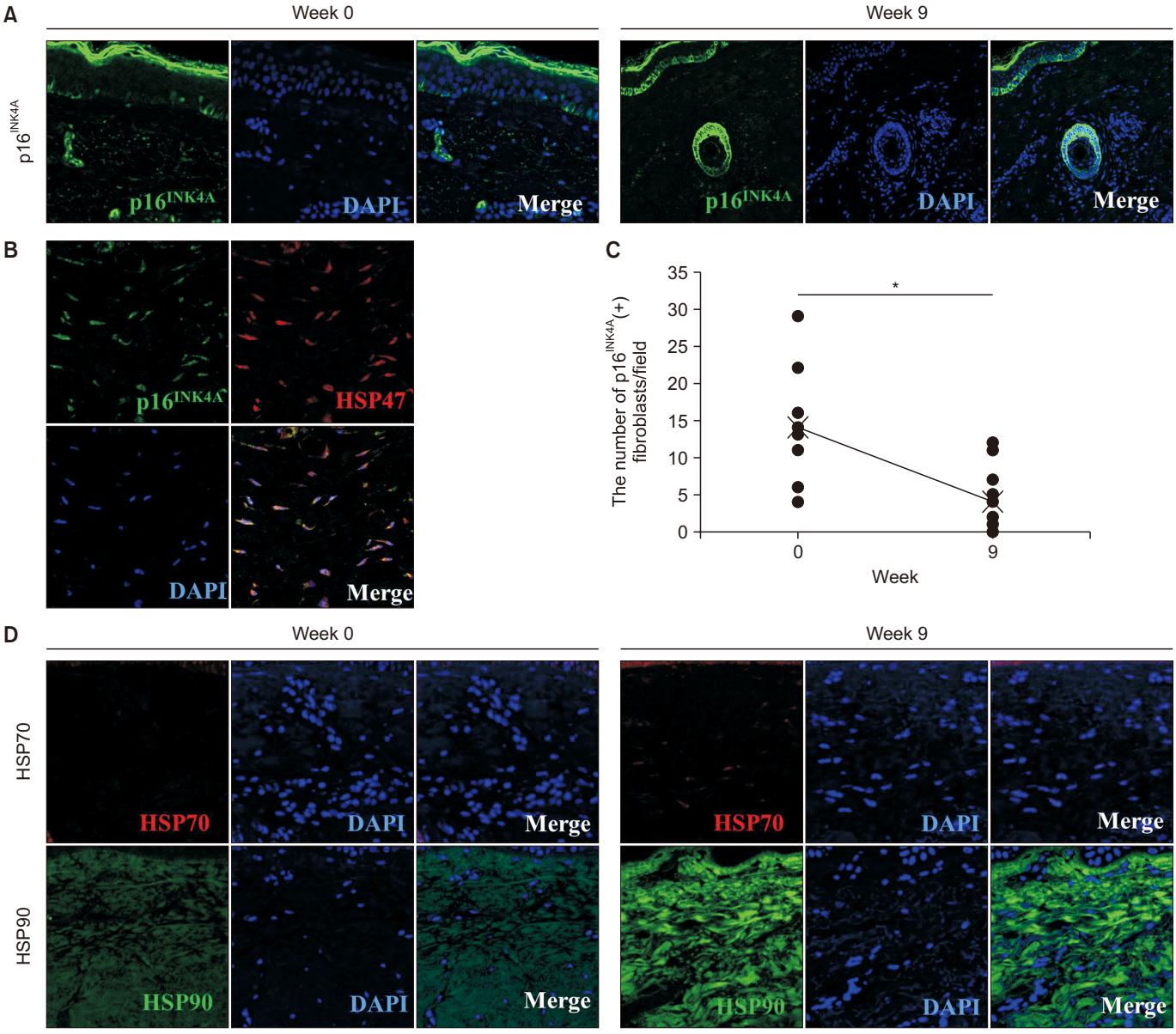

Fig. 4. Radiofrequency (RF) treatment reduced the number of senescent fibroblasts and up-regulated the expression of heat shock protein (HSP) 70 and HSP90 in melasma. (A) The presence of $p16^{INK4A}$-positive cells before and after RF treatment. Original magnification ×200. (B) Double immunostaining for $p16^{INK4A}$ and HSP47 indicated that the senescent cells were fibroblasts. Original magnification ×400. (C) The mean number of $p16^{INK4A}$-positive fibroblasts per field decreased from 14.1 to 4.4 after treatment. (D) The expression of HSP70 and HSP90 before and after RF treatment. Original magnification ×400. *Statistically significance ($p<0.05$).

environment. In this study, we revealed that continuous thermal stimulation of skin to the temperature of 43°C using the temperature-controlled continuous non-invasive RF device appears to remodel the dermal environment in melasma, leading to reduced pigmentation. We showed that there is a decreased number of $p16^{INK4A}$-positive senescent fibroblasts after the RF treatment. The change in the fibroblasts population might result in the restoration of basement membrane, and increased secretion of SDF-1, which all could contribute to the inhibition of the melanogenic process.

The mechanism behind the reduced number of senescent fibroblasts after the RF treatment has not been fully elucidated to date. We hypothesized that the thermal damage by RF treatment induces rejuvenation of senescent fibroblasts. Repetitive mild heat shock (40°C~42°C for 30~60 minutes) suppresses age-related morphologic changes of fibroblasts and elongates

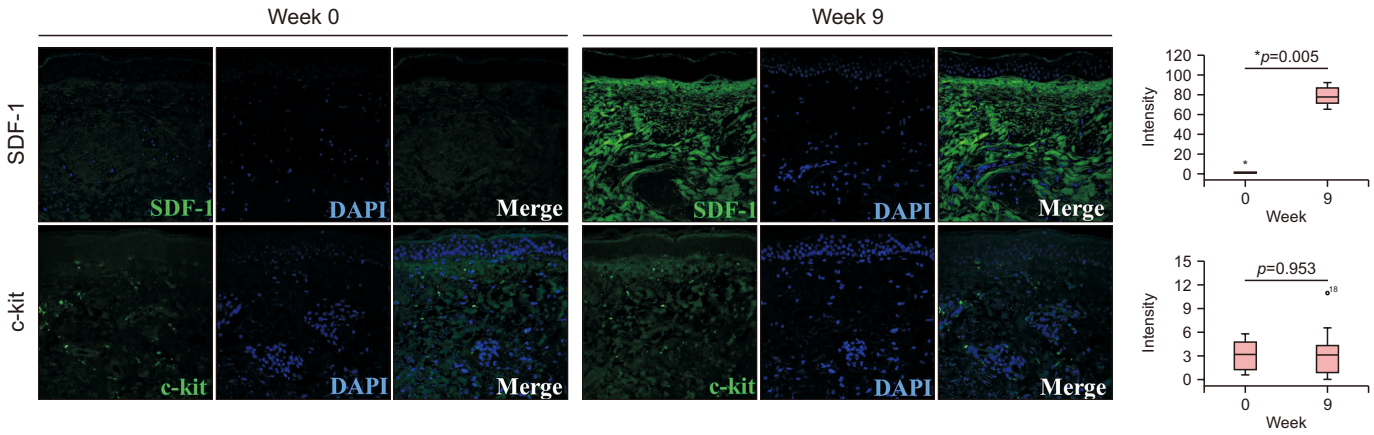

Fig. 5. Radiofrequency (RF) induced the secretion of stromal derived factor-1 (SDF-1). In contrast, immunostaining for the c-kit showed no significant change after the RF treatment. Original magnification ×200. *Statistically significance ($p<0.05$).

cellular longevity by 20% *in vitro*[25,26]. This rejuvenating process of fibroblasts is achieved by the activation of the ERK pathway, which is involved in cellular survival and proliferation[27]. Heat shock also stimulates the translocation of the heat shock transcription factor into the nucleus, and thus the expression of HSP70 and HSP90, which act as chaperones, is involved in the renaturation of unfolded proteins[28]. In addition, heat shock also induces several cellular responses, including antioxidant response, DNA damage response, and unfolded protein response, to achieve homeostasis[29-32]. The removal of abnormal intracellular protein and suppression of reactive oxygen species production occur as a consequence, which results in delayed aging of fibroblasts.

In the present study, we showed the restoration of basement membrane after the RF treatment. Disruption of basement membrane is a common histologic finding in melasma, observed in 83% to 95.5% of melasma patients[33]. Disrupted basement membrane could induce a descent of melanocytes, resulting in pendulous melanocytes observed in melasma[34]. In a cell culture model of normal human melanocytes (NHMs) on three dimensional (3D) Matrigel—a basement membrane-like extracellular matrix extract—the intracellular melanin level was significantly lower when compared with NHMs cultured on gelatin-coated 2D plate or 3D collagen gel[35]. Under UV radiation, increase expression of heparanase causes degradation of heparan sulfate at the basement membrane, which results in enhanced diffusion of fibroblast-derived melanogenic growth factors from dermis to epidermis through the dermo-epidermal junction, thereby promotes melanogenesis[36].

SDF-1, which is also known as C-X-C motif chemokine ligand 12 (CXCL12), binds to the C-X-C chemokine receptor type 4 (CXCR4) to activate several downstream signaling pathways, while blocking the adenylate cyclase and cAMP production[37,38]. Recently, SDF-1 has been highlighted as a mediator for senescent fibroblast-induced pigmentation. Reduced secretion of SDF-1 from the senescent fibroblasts of senile lentigo was shown to promote pigmentation, which was reversed when senescent fibroblasts were removed by the microneedle RF treatment[17]. Our result suggests that senescent fibroblasts and SDF-1 are involved in the pathogenesis of both melasma and senile lentigo, despite having distinct clinical presentation and histological characteristics[4].

Fibroblasts are known to secrete several melanogenic growth factors, including SCF, bFGF, and HGF[23]. The expression of SCF, HGF, and keratinocyte growth factor was observed in senile lentigo skin, and their secretion was induced by the photoaging of fibroblasts[39]. We examined the c-kit—the receptor of SCF—to explain the anti-melanogenic effect of RF. SCF, which binds with the c-kit to activate the MAPK/ERK pathway, is known as a potent melanogenic cytokine secreted from senescent fibroblasts[16,23]. An up-regulated expression of the c-kit on melanocytes and SCF in the dermis was reported in melasma skin[24]. However, there was no significant difference in the expression of c-kit after the RF treatment in our study. Different from the SDF-1, which is secreted from fibroblasts, SCF is secreted not only from fibroblasts, but also from keratinocytes in response to various stimuli, such as UV irradiation[40]. Possible explanation is that the secretion SCF from keratinocytes is not affected by the RF treatment though its secretion from fibroblasts is decreased by eliminating senescent fibroblasts.

In conclusion, skin heating by the temperature-controlled continuous non-invasive RF device improved melasma via reduced number of senescent fibroblasts, increased expression of HSP70 and HSP90, restoration of basement membrane, and up-regulated secretion of SDF-1.

CONFLICTS OF INTEREST

The authors have nothing to disclose.

FUNDING SOURCE

None.

DATA SHARING STATEMENT

The data that support the findings of this study are available from the corresponding author upon reasonable request.

ORCID

Soon-Hyo Kwon, https://orcid.org/0000-0002-7295-5725
Jung-Im Na, https://orcid.org/0000-0002-5717-2490
Chang-Hun Huh, https://orcid.org/0000-0003-3944-7777
Kyoung-Chan Park, https://orcid.org/0000-0002-1588-3307

REFERENCES

1. Newcomer VD, Lindberg MC, Sternberg TH. A melanosis of the face ("chloasma"). Arch Dermatol 1961;83:284-299.
2. Lee AY. Recent progress in melasma pathogenesis. Pigment Cell Melanoma Res 2015;28:648-660.
3. Passeron T, Picardo M. Melasma, a photoaging disorder. Pigment Cell Melanoma Res 2018;31:461-465.
4. Kwon SH, Na JI, Choi JY, Park KC. Melasma: updates and perspectives. Exp Dermatol 2019;28:704-708.
5. Kwon SH, Hwang YJ, Lee SK, Park KC. Heterogeneous pathology of melasma and its clinical implications. Int J Mol Sci 2016;17:824.
6. Gupta AK, Gover MD, Nouri K, Taylor S. The treatment of melasma: a review of clinical trials. J Am Acad Dermatol 2006;55:1048-1065.
7. Yamaguchi Y, Itami S, Watabe H, Yasumoto K, Abdel-Malek ZA, Kubo T, et al. Mesenchymal-epithelial interactions in the skin: increased expression of dickkopf1 by palmoplantar fibroblasts inhibits melanocyte growth and differentiation. J Cell Biol 2004;165:275-285.
8. Yamaguchi Y, Passeron T, Watabe H, Yasumoto K, Rouzaud F, Hoashi T, et al. The effects of dickkopf 1 on gene expression and Wnt signaling by melanocytes: mechanisms underlying its suppression of melanocyte function and proliferation. J Invest Dermatol 2007;127:1217-1225.
9. Choi W, Wolber R, Gerwat W, Mann T, Batzer J, Smuda C, et al. The fibroblast-derived paracrine factor neuregulin-1 has a novel role in regulating the constitutive color and melanocyte function in human skin. J Cell Sci 2010;123(Pt 18):3102-3111.
10. Choi W, Kolbe L, Hearing VJ. Characterization of the bioactive motif of neuregulin-1, a fibroblast-derived paracrine factor that regulates the constitutive color and the function of melanocytes in human skin. Pigment Cell Melanoma Res 2012;25:477-481.
11. Kim M, Han JH, Kim JH, Park TJ, Kang HY. Secreted frizzled-related protein 2 (sFRP2) functions as a melanogenic stimulator; the role of sFRP2 in UV-induced hyperpigmentary disorders. J Invest Dermatol 2016;136:236-244.
12. Kim JY, Lee TR, Lee AY. Reduced WIF-1 expression stimulates skin hyperpigmentation in patients with melasma. J Invest Dermatol 2013;133:191-200.
13. Byun JW, Park IS, Choi GS, Shin J. Role of fibroblast-derived factors in the pathogenesis of melasma. Clin Exp Dermatol 2016;41:601-609.
14. Duval C, Cohen C, Chagnoleau C, Flouret V, Bourreau E, Bernerd F. Key regulatory role of dermal fibroblasts in pigmentation as demonstrated using a reconstructed skin model: impact of photo-aging. PLoS One 2014;9:e114182.
15. Waldera Lupa DM, Kalfalah F, Safferling K, Boukamp P, Poschmann G, Volpi E, et al. Characterization of skin aging-associated secreted proteins (SAASP) produced by dermal fibroblasts isolated from intrinsically aged human skin. J Invest Dermatol 2015;135:1954-1968.
16. Shin J, Kim JH, Kim EK. Repeated exposure of human fibroblasts to UVR induces secretion of stem cell factor and senescence. J Eur Acad Dermatol Venereol 2012;26:1577-1580.
17. Yoon JE, Kim Y, Kwon S, Kim M, Kim YH, Kim JH, et al. Senescent fibroblasts drive ageing pigmentation: a potential therapeutic target for senile lentigo. Theranostics 2018;8:4620-4632.
18. Kwon HH, Choi SC, Jung JY, Park GH. Combined treatment of melasma involving low-fluence Q-switched Nd:YAG laser and fractional microneedling radiofrequency. J Dermatolog Treat 2019;30:352-356.
19. Jung JW, Kim WO, Jung HR, Kim SA, Ryoo YW. A face-split study to evaluate the effects of microneedle radiofrequency with Q-switched Nd:YAG laser for the treatment of melasma. Ann Dermatol 2019;31:133-138.
20. Jensen EC. Quantitative analysis of histological staining and fluores-

cence using ImageJ. Anat Rec (Hoboken) 2013;296:378-381.
21. Baker DJ, Wijshake T, Tchkonia T, LeBrasseur NK, Childs BG, van de Sluis B, et al. Clearance of p16Ink4a-positive senescent cells delays ageing-associated disorders. Nature 2011;479:232-236.
22. Ito S, Nagata K. Biology of Hsp47 (Serpin H1), a collagen-specific molecular chaperone. Semin Cell Dev Biol 2017;62:142-151.
23. Imokawa G, Yada Y, Morisaki N, Kimura M. Biological characterization of human fibroblast-derived mitogenic factors for human melanocytes. Biochem J 1998;330(Pt 3):1235-1239.
24. Kang HY, Hwang JS, Lee JY, Ahn JH, Kim JY, Lee ES, et al. The dermal stem cell factor and c-kit are overexpressed in melasma. Br J Dermatol 2006;154:1094-1099.
25. Rattan SI. Repeated mild heat shock delays ageing in cultured human skin fibroblasts. Biochem Mol Biol Int 1998;45:753-759.
26. Nielsen ER, Eskildsen-Helmond YE, Rattan SI. MAP kinases and heat shock-induced hormesis in human fibroblasts during serial passaging in vitro. Ann N Y Acad Sci 2006;1067:343-348.
27. Jang YH, Koo GB, Kim JY, Kim YS, Kim YC. Prolonged activation of ERK contributes to the photorejuvenation effect in photodynamic therapy in human dermal fibroblasts. J Invest Dermatol 2013;133:2265-2275.
28. Rattan SI. Hormetic mechanisms of anti-aging and rejuvenating effects of repeated mild heat stress on human fibroblasts in vitro. Rejuvenation Res 2004;7:40-48.
29. Rattan SIS, Demirovic D, Nizard C. A preliminary attempt to establish multiple stress response profiles of human skin fibroblasts exposed to mild or severe stress during ageing in vitro. Mech Ageing Dev 2018;170:92-97.
30. Verbeke P, Clark BF, Rattan SI. Reduced levels of oxidized and glycoxidized proteins in human fibroblasts exposed to repeated mild heat shock during serial passaging in vitro. Free Radic Biol Med 2001;31:1593-1602.
31. Verbeke P, Deries M, Clark BF, Rattan SI. Hormetic action of mild heat stress decreases the inducibility of protein oxidation and glycoxidation in human fibroblasts. Biogerontology 2002;3:117-120.
32. Fonager J, Beedholm R, Clark BF, Rattan SI. Mild stress-induced stimulation of heat-shock protein synthesis and improved functional ability of human fibroblasts undergoing aging in vitro. Exp Gerontol 2002;37:1223-1228.
33. Torres-Álvarez B, Mesa-Garza IG, Castanedo-Cázares JP, Fuentes-Ahumada C, Oros-Ovalle C, Navarrete-Solis J, et al. Histochemical and immunohistochemical study in melasma: evidence of damage in the basal membrane. Am J Dermatopathol 2011;33:291-295.
34. Kim H, Kim HJ, Lee K, Kim JM, Kim HS, Kim JR, et al. α-lipoic acid attenuates vascular calcification via reversal of mitochondrial function and restoration of Gas6/Axl/Akt survival pathway. J Cell Mol Med 2012;16:273-286.
35. Choi H, Jin SH, Han MH, Lee J, Ahn S, Seong M, et al. Human melanocytes form a PAX3-expressing melanocyte cluster on Matrigel by the cell migration process. J Dermatol Sci 2014;76:60-66.
36. Iriyama S, Ono T, Aoki H, Amano S. Hyperpigmentation in human solar lentigo is promoted by heparanase-induced loss of heparan sulfate chains at the dermal-epidermal junction. J Dermatol Sci 2011;64:223-228.
37. Teixidó J, Martínez-Moreno M, Díaz-Martínez M, Sevilla-Movilla S. The good and bad faces of the CXCR4 chemokine receptor. Int J Biochem Cell Biol 2018;95:121-131.
38. Ruiz EJ, Oeztuerk-Winder F, Ventura JJ. A paracrine network regulates the cross-talk between human lung stem cells and the stroma. Nat Commun 2014;5:3175.
39. Kovacs D, Cardinali G, Aspite N, Cota C, Luzi F, Bellei B, et al. Role of fibroblast-derived growth factors in regulating hyperpigmentation of solar lentigo. Br J Dermatol 2010;163:1020-1027.
40. Morita E, Lee DG, Sugiyama M, Yamamoto S. Expression of c-kit ligand in human keratinocytes. Arch Dermatol Res 1994;286:273-277.